

ANALYSIS OF FEL OSCILLATIONS IN A PERFECTLY SYNCHRONIZED OPTICAL CAVITY

N. Nishimori*, JAEA, Ibaraki, Japan.

Abstract

We analyze free-electron-laser (FEL) oscillations in a perfectly synchronized optical cavity by solving the one-dimensional FEL equations. The radiation stored in the cavity can finally evolve into an intense few-cycle optical pulse in the high-gain and low-loss regime. The evolution of the leading slope of the optical pulse, which is defined from the front edge toward the primary peak, is found to play an important role in generating the intense few-cycle pulse. The phase space evolution of electrons on the second pass which interact with the leading slope of a SASE output pulse is obtained in a perturbation method similar to that used in our previous study for a SASE FEL. The resulting analytical solution of the leading slope in the second pass is shown to be approximated by that of a SASE FEL with FEL parameter greater than ρ . The same perturbation method can thus be used to the subsequent passes.

INTRODUCTION

The FEL dynamics is affected by the slippage that is caused by the velocity difference between the electron bunch and the optical pulse inside an undulator. The group velocity of the optical pulse becomes slightly slower than the vacuum speed of light, since the trailing slope of the optical pulse is mainly amplified due to the slippage. This phenomenon, called the laser lethargy (see Ref. [1] and references therein), can be compensated in oscillators by slightly shortening the optical cavity length from the perfect synchronism ($\delta L = 0$), where the cavity length exactly matches with the injection period of the electron bunches. The FEL dynamics of the oscillators with shorter cavity length ($\delta L < 0$) has been studied extensively [2, 3]. At $\delta L = 0$, the optical pulse centroid continues to be retarded on successive passes through the undulator, and the optical pulse finally dissipates, as shown in theoretical studies [4, 5, 6].

An experiment of a high-power FEL driven by a superconducting linac in the Japan Atomic Energy Research Institute (JAERI) FEL facility has however showed that an intense, ultrashort optical pulse is generated at $\delta L = 0.0 \pm 0.1 \mu\text{m}$ despite the lethargy [7, 8]. The optical power curve measured with respect to δL is well reproduced by the time-dependent simulation code based on one-dimensional (1D) FEL equations [9], if shot-noise effect is included in every fresh electron bunch. A few theoretical studies have attempted to explain the FEL oscillations at $\delta L = 0$, proposing that sideband instability [10] or superradiance in short-pulse FELs [11] is the fundamental physics responsi-

ble for the lasing at $\delta L = 0$. Nevertheless, the underlying physics responsible for the FEL oscillations at $\delta L = 0$ has not been clearly explained yet.

In this paper, we investigate the FEL evolution at $\delta L = 0$ by analytically solving the 1D FEL equations. A set of nondimensional parameters and the 1D FEL equations used in Ref. [12] are employed for the present study. The optical pulse on the first pass, which is equivalent to the output of a self-amplified spontaneous-emission (SASE) FEL and represented by the solution of the cubic equation [14, 15, 16], is reflected back into the undulator for subsequent amplifications in FEL oscillators. The phase space evolution of electrons on the second pass which interact with the leading slope of the FEL pulse, which is defined from the front edge toward the primary peak amplitude in the present paper, is obtained in a perturbation method similar to that used in our previous work for the phase space evolution of electrons in a SASE FEL [12]. Consequently, an analytical solution for the optical growth of the leading slope during the second pass is derived. The leading slope of the output pulse is shown to be approximated by that of a SASE FEL with FEL parameter greater than ρ . The same process can thus be applied to pass numbers greater than $n = 2$ and the evolution of the leading slope with respect to n is obtained analytically. The output field similar to that of a SASE FEL accounts for the exponential increase of the field amplitude in the leading slope from the front edge toward the primary peak, and the amplitude gradient with respect to the longitudinal position is shown to increase with n . With the increasing gradient, the field gain per pass decreases down to the level of optical cavity loss α , and a self-similar radiation pulse is generated at saturation. The evolution of the leading slope leads to sustained FEL oscillations at $\delta L = 0$ and thus disappearance of the lethargy effect. More details are described in Ref. [13].

1D FEL EQUATIONS

The dimensionless 1D FEL equations of Colson are used in the present study under the slowly varying envelope approximation [17], while the variables used here are similar to Bonifacio's variables [16]. The simplest situation is considered in the present study. The electron beam energy is given by $\gamma_0 mc^2$ with small energy spread. The initial electron bunch has a rectangular shape with density of n_e and a uniform distribution in phase. The fundamental FEL parameter in MKSA units is given by

$$\rho = \frac{1}{\gamma_0} [ea_w F \sqrt{n_e / (\epsilon_0 m)} / (4ck_w)]^{2/3}. \quad (1)$$

Here $\lambda_w = 2\pi/k_w$ is the period of the undulator, a_w is the undulator parameter, and F is unity for a helical undulator

* nishimori.nobuyuki@jaea.go.jp

or Bessel function $[J J]$ for a planar undulator [16]. The dimensionless time is defined by $\tau = 4\pi\rho ct/\lambda_w$, so that $\delta\tau = 1$ corresponds to the transit time of light through one gain length of $\lambda_w/(4\pi\rho)$. The longitudinal position of the i th electron is defined by $\zeta_i(\tau) = 4\pi\rho[z_i(t) - ct]/\lambda_r$, so that $\delta\zeta = 1$ corresponds to the cooperation length defined by $L_c = \lambda_r/(4\pi\rho)$. Here $\lambda_r = \lambda_w(1 + a_w^2)/(2\gamma_0^2)$ is the resonant wavelength. The dimensionless field envelope is defined by

$$a(\zeta, \tau) = \frac{2\pi e a_w \lambda_w F}{(4\pi\rho)^2 \gamma_0^2 m c^2} E(\zeta, \tau) \exp[i\phi(\zeta, \tau)], \quad (2)$$

with phase $\phi(\zeta, \tau)$, which is equivalent to Bonifacio's envelope [16]. Here $E(\zeta, \tau)$ is the rms optical field strength. The dimensionless energy and phase of the i th electron are respectively defined by $\mu_i(\tau) = [\gamma_i(t) - \gamma_0]/(\rho\gamma_0)$ and $\psi_i(\tau) = (k_w + k_r)z_i(t) - \omega_r t$, where $k_r = 2\pi/\lambda_r$ is the wave number of the resonant wavelength λ_r . The dimensionless energy $\mu_i(\tau)$ also means the dimensionless energy change at τ from $\tau = 0$, since the energy spread of the initial electron beam is assumed to be small, i.e., $\mu_i(0) = 0$.

In the present definition, the evolutions of the field envelope $a(\zeta, \tau)$, the energy $\mu_i(\tau)$ and phase $\psi_i(\tau)$ of the i th electron during FEL interaction are respectively given by [5]

$$\frac{d\mu_i(\tau)}{d\tau} = a[\zeta_i(\tau), \tau] \exp[i\psi_i(\tau)] + \text{c.c.}, \quad (3)$$

$$\frac{d\psi_i(\tau)}{d\tau} = \mu_i(\tau), \quad (4)$$

$$\frac{\partial a(\zeta, \tau)}{\partial \tau} = -\langle \exp[-i\psi_i(\tau)] \rangle_{\zeta_i(\tau)=\zeta}. \quad (5)$$

The angular bracket indicates the average of all the electrons in the volume V around ζ .

EVOLUTION OF SASE FEL PULSE

The optical field and electron phase space evolutions on the first pass, which are equivalent to those in a SASE FEL, are presented in our previous work [12]. The startup process known as spectrum narrowing [18] or as longitudinal phase mixing [19] leads to a uniform field in time and space. The phase of the field $\phi(0)$ is almost uniform over the length $N\lambda_r$ along the propagation direction when the incident electron beam passes through N undulator periods [5, 19]. In the present study, the initial uniform field is assumed to be given by $|a(0)|e^{i\phi(0)}$ for simplicity. The initial field evolves through electric interaction with undulating electrons as it passes through the undulator. The incident electron beam is assumed to be uniformly distributed in phase $\psi_i(0)$ with resonant energy $\mu_i(0) = 0$ and interacts with the SASE FEL field in the steady-state region due to the slippage [16]. The evolution of the uniform field as a function of time is derived from Eqs. (3), (4), and (5), as described by Colson *et al.* in Ref. [15].

The electron phase can be expressed as $\psi_i(\tau) = \psi_i(0) + \Delta\psi_i(\tau)$ where $\Delta\psi_i(\tau)$ is the first-order perturbation in

$a(\tau)$. The field at time τ for the steady-state region where $\zeta < -\tau$ is given by

$$a(\tau) = a(0) + i \int_0^\tau \langle e^{-i\psi_i(0)} \Delta\psi_i(\tau') \rangle_{\zeta_i(\tau)=\zeta} d\tau'. \quad (6)$$

The i th electron interacts with the field in the steady-state region due to the slippage, and the energy modulation at τ' during $\delta\tau'$ is given from Eq. (3) by $\delta\mu_i(\tau') = [a(\tau')e^{i\psi_i(0)} + \text{c.c.}] \delta\tau'$. The energy change of the i th electron at time τ , $\mu_i(\tau)$, is given by the sum of those modulations during τ :

$$\mu_i(\tau) = \int_0^\tau \{a(\tau')e^{i\psi_i(0)} + \text{c.c.}\} d\tau'. \quad (7)$$

The electron phase perturbation is given from Eq. (4) by

$$\Delta\psi_i(\tau) = \int_0^\tau \mu_i(\tau') d\tau' \quad (8)$$

$$= \int_0^\tau d\tau' \int_0^{\tau'} \{a(\tau'') \exp[i\psi_i(0)] + \text{c.c.}\} d\tau'' \quad (9)$$

Substitution of Eq. (9) into Eq. (6) leads to

$$a(\tau) = a(0) + i \int_0^\tau d\tau' \int_0^{\tau'} d\tau'' \int_0^{\tau''} a(\tau''') d\tau'''. \quad (10)$$

The integral equation (10) can be written in a differential form by taking successive derivatives. The solution is expressed in the form $a(\tau) = \sum_{n=1}^3 a_n \exp(\alpha_n \tau)$ where the α_n are three complex roots of the cubic equation $\alpha^3 = i$ [14, 15, 16]. When the initial conditions $\dot{a}(0) = \ddot{a}(0) = 0$, the field at time τ for the steady-state region where $\zeta < -\tau$ is given by

$$a(\tau) = \frac{|a(0)|e^{i\phi(0)}}{3} \left(e^{\tau} e^{i\pi/6} + e^{-\tau} e^{-i\pi/6} + e^{\tau} e^{-i\pi/2} \right). \quad (11)$$

Equation (11) is valid in the linear regime before saturation when the incident electron beam is resonant.

EVOLUTION OF OSCILLATOR FEL PULSE

We first study the optical field and electron phase space evolutions on the second pass ($n = 2$) in an analytical way and then show that the analytical method can be applied to the n th pass with reasonable approximations. At first the notation n is thus used for $n = 2$.

FEL evolution on the second pass

The input field for the second pass, $a_n(\zeta) = a_n(\zeta, 0)$, is the same as the output of a SASE FEL with FEL parameter ρ except for a decrease of the amplitude due to the cavity loss α . The leading slope of the input field for the second pass is therefore given as a function of ζ by

$$a_n(\zeta) = (|a_n(0)|e^{i\phi_n(0)}/3) \left(e^{-\rho_n \zeta} e^{i\pi/6} + e^{\rho_n \zeta} e^{-i\pi/6} + e^{-\rho_n \zeta} e^{-i\pi/2} \right), \quad (12)$$

where $\rho_2 = 1$ and $|a_2(0)| \approx (1 - \alpha/2)|a(0)|$. Equation (12) can be used where $|\zeta| < L_s$ and $|\zeta| < L_b$ before the field reaches saturation. Here L_b is the incident electron bunch length in units of L_c and $L_s = 4\pi\rho N_w$ is the slippage distance. The phase space evolution of electrons during interaction with the leading slope given by Eq. (12) is quite similar to that of a SASE FEL. The perturbation method used in Ref. [12] can be applied to a study of the optical growth during the second pass, as long as the growth is small and the field $a_n(\zeta)$ remains almost unchanged during the FEL interaction. The electron phase can be expressed as $\psi_i(\tau) = \psi_i(0) + \Delta\psi_i(\tau)$ where $\Delta\psi_i(\tau)$ is the first-order perturbation in $a_n[\zeta_i(\tau)]/\rho_n^2$, since the field in the leading slope divided by ρ_n^2 is weak even after saturation except for a narrow range near ζ_p . When the i th electron is modulated in energy by interacting with the leading slope, the energy modulation at τ' during $\delta\tau'$ is expressed from Eq. (3) by $\delta\mu_i(\tau') = \{a_n[\zeta_i(\tau')]e^{i\psi_i(0)} + \text{c.c.}\}\delta\tau'$. The energy change of the i th electron at time τ , $\mu_i(\tau)$, is given by the sum of those modulations during τ :

$$\mu_i(\tau) = \int_0^\tau \{a_n[\zeta_i(\tau')] \exp[i\psi_i(0)] + \text{c.c.}\} d\tau'. \quad (13)$$

The integration of Eq. (13) after substitution of Eq. (12) yields

$$\begin{aligned} \mu_i(\tau) = & [2|a_n(0)|/3\rho_n] \times \\ & \{e^{-\sqrt{3}\rho_n\zeta_i(\tau)/2} \cos[\psi_i(0) + \phi_n(0) - \rho_n\zeta_i(\tau)/2 - \pi/6] \\ & - e^{-\sqrt{3}\rho_n\zeta_i(0)/2} \cos[\psi_i(0) + \phi_n(0) - \rho_n\zeta_i(0)/2 - \pi/6] \\ & - e^{\sqrt{3}\rho_n\zeta_i(\tau)/2} \cos[\psi_i(0) + \phi_n(0) - \rho_n\zeta_i(\tau)/2 + \pi/6] \\ & + e^{\sqrt{3}\rho_n\zeta_i(0)/2} \cos[\psi_i(0) + \phi_n(0) - \rho_n\zeta_i(0)/2 + \pi/6] \\ & + \cos[\psi_i(0) + \phi_n(0) + \rho_n\zeta_i(\tau) + \pi/2] \\ & - \cos[\psi_i(0) + \phi_n(0) + \rho_n\zeta_i(0) + \pi/2]\}. \end{aligned} \quad (14)$$

The integration of Eq. (8) after substitution of Eq. (14) yields

$$\begin{aligned} \Delta\psi_i(\tau) = & [2|a_n(0)|/3\rho_n^2] \times \\ & \{e^{-\sqrt{3}\rho_n\zeta_i(\tau)/2} \cos[\psi_i(0) + \phi_n(0) - \rho_n\zeta_i(\tau)/2 - \pi/3] \\ & - e^{-\sqrt{3}\rho_n\zeta_i(0)/2} \cos[\psi_i(0) + \phi_n(0) - \rho_n\zeta_i(0)/2 - \pi/3] \\ & - \rho_n\tau e^{-\sqrt{3}\rho_n\zeta_i(0)/2} \cos[\psi_i(0) + \phi_n(0) - \rho_n\zeta_i(0)/2 - \pi/6] \\ & + e^{\sqrt{3}\rho_n\zeta_i(\tau)/2} \cos[\psi_i(0) + \phi_n(0) - \rho_n\zeta_i(\tau)/2 + \pi/3] \\ & - e^{\sqrt{3}\rho_n\zeta_i(0)/2} \cos[\psi_i(0) + \phi_n(0) - \rho_n\zeta_i(0)/2 + \pi/3] \\ & + \rho_n\tau e^{\sqrt{3}\rho_n\zeta_i(0)/2} \cos[\psi_i(0) + \phi_n(0) - \rho_n\zeta_i(0)/2 + \pi/6] \\ & - \cos[\psi_i(0) + \phi_n(0) + \rho_n\zeta_i(\tau)] \\ & + \cos[\psi_i(0) + \phi_n(0) + \rho_n\zeta_i(0)] \\ & - \rho_n\tau \cos[\psi_i(0) + \phi_n(0) + \rho_n\zeta_i(0) + \pi/2]\}, \end{aligned} \quad (15)$$

where $\zeta_i(\tau) = \zeta_i(0) - \tau$ is used, which is valid as long as the electron energy change $\mu_i(\tau)$ is small and $d\zeta_i(\tau)/d\tau = -1$ holds. Equations (14) and (15) represent the phase space evolution of the i th electron during the second pass.

The field gain $da_n(\zeta)/d\tau$ caused by the electron microbunch in units of λ_r whose initial position is $\zeta_i(0) = \zeta + \tau$ is derived from substitution of $\psi_i(\tau) = \psi_i(0) + \Delta\psi_i(\tau)$ into Eq. (5) as follows:

$$\begin{aligned} da_n(\zeta)/d\tau = & (|a_n(0)|e^{i\phi_n(0)}/3\rho_n^2) \\ & \times \{e^{(-\rho_n\zeta e^{i\pi/6} + i\pi/6)} [1 - e^{-\rho_n\tau e^{i\pi/6}} (1 + \rho_n\tau e^{i\pi/6})] \\ & - e^{(\rho_n\zeta e^{-i\pi/6} - i\pi/6)} [1 - e^{\rho_n\tau e^{-i\pi/6}} (1 - \rho_n\tau e^{-i\pi/6})] \\ & + e^{(-\rho_n\zeta e^{-i\pi/2} - i\pi/2)} [1 - e^{-\rho_n\tau e^{-i\pi/2}} (1 + \rho_n\tau e^{-i\pi/2})]\}, \end{aligned} \quad (16)$$

when $|\Delta\psi_i(\tau)| \ll 1$.

The field $a_n(\zeta)$ is sequentially amplified from $\tau = 0$ to $\tau = -\zeta$ by the electron microbunches whose initial position are $\zeta_i(0) = \zeta + \tau$ as it passes through the undulator. The field gain per pass is given by

$$\begin{aligned} da_n(\zeta)/dn = & [|a_n(0)|e^{i\phi_n(0)}/3\rho_n^3] \\ & \times \{-\rho_n\zeta [e^{(-\rho_n\zeta e^{i\pi/6} + i\pi/6)} - e^{(\rho_n\zeta e^{-i\pi/6} - i\pi/6)} \\ & + e^{(-\rho_n\zeta e^{-i\pi/2} - i\pi/2)}] - 2[e^{(-\rho_n\zeta e^{i\pi/6})} + e^{(\rho_n\zeta e^{-i\pi/6})} \\ & + e^{(-\rho_n\zeta e^{-i\pi/2})}] + 6\}. \end{aligned} \quad (17)$$

The leading slope of the output field for the second pass is thus given by

$$\begin{aligned} a_n(\zeta) + da_n(\zeta)/dn = & [|a_n(0)|e^{i\phi_n(0)}/3\rho_n^3] \\ & \times \{-\rho_n\zeta [e^{(-\rho_n\zeta e^{i\pi/6} + i\pi/6)} - e^{(\rho_n\zeta e^{-i\pi/6} - i\pi/6)} \\ & + e^{(-\rho_n\zeta e^{-i\pi/2} - i\pi/2)}] + (\rho_n^3 - 2)[e^{(-\rho_n\zeta e^{i\pi/6})} \\ & + e^{(\rho_n\zeta e^{-i\pi/6})} + e^{(-\rho_n\zeta e^{-i\pi/2})}] + 6\}. \end{aligned} \quad (18)$$

The amplitude and phase of the output field given by Eq. (18) are plotted as solid circles in Figs. 1(a) and 1(b), respectively, as a function of ζ . The solid line shows the output field of the second pass obtained in a time-dependent numerical calculation, which solves Eqs. (3)–(5) with an input field given by Eq. (12) with $\rho_n = 1$ and represented by the dotted line. In the calculation, the shot-noise effect is neglected. One can see that the field given by Eq. (18) agrees well with the numerical calculation where $|\zeta| < 3.5$ but the phase gradually deviates from the calculation where $|\zeta| \geq 3.5$. This is because the assumption that the field remains almost unchanged during the passage through an undulator does no longer hold where $|\zeta| \geq 3.5$ for the second pass.

FEL evolution on pass numbers greater than 2

The output field of the second pass is equivalent to the input field for the third pass except for amplitude decrease due to the optical cavity loss α . If the input field for the third pass is found to be approximated by Eq. (12), the same procedure described in the previous subsection can be used for a study of the optical growth during the third pass. The dash-dotted line in Fig. 1 shows the field given by Eq. (12) with $\rho_n = 1.28$. The amplitude of this field is different from that obtained in a numerical calculation

(solid line) by only 10% to -20% where $|\zeta| < 5$, and the phase is different from the numerical calculation by only ± 0.17 rad. These results suggest that the input field for the third pass can be approximated by Eq. (12) with $\rho_3 = 1.28$. In a similar way, one can obtain ρ_n of the input field for pass numbers greater than $n = 3$ as well. For example $\rho_4 = 1.52$, $\rho_5 = 1.73$, $\rho_6 = 1.90$, and $\rho_7 = 2.05$.

As ρ_n increases, $\rho_n^3 - 2 \sim \rho_n^3$ and Eq. (18) asymptotically approaches

$$a_n(\zeta) + da_n(\zeta)/dn \sim a_n(\zeta) + [|a_n(0)|e^{i\phi_n(0)}/3\rho_n^3] \times \{-\rho_n\zeta[e^{-\rho_n\zeta e^{i\pi/6} + i\pi/6} - e^{\rho_n\zeta e^{-i\pi/6} - i\pi/6}] + e^{(-\rho_n\zeta e^{-i\pi/2} - i\pi/2)}\}, \quad (19)$$

The field evolution per pass can also be obtained by differentiation of Eq. (12) with respect to the pass number n under the assumption that ρ_n is independent of ζ as follows:

$$da_n(\zeta)/dn = (|a_n(0)|e^{i\phi_n(0)}/3)(d\rho_n/dn) \times \{-\zeta[e^{-\rho_n\zeta e^{i\pi/6} + i\pi/6} - e^{\rho_n\zeta e^{-i\pi/6} - i\pi/6}] + e^{(-\rho_n\zeta e^{-i\pi/2} - i\pi/2)}\}. \quad (20)$$

Equation (20) should be equal to Eq. (19) subtracted by $a_n(\zeta)$ as long as the gain is much higher than the optical cavity loss and ρ_n is large enough for Eq. (19) to hold. This yields

$$d\rho_n/dn = 1/\rho_n^2. \quad (21)$$

When we assume that Eq. (19) holds when $\rho_n > 2$, Eq. (21) gives

$$\rho_n \approx (3n - 12)^{1/3} \quad (22)$$

for $n \geq 7$. Substitution of Eq. (22) into Eq. (20) yields

$$(1/|a_n(\zeta)|)(d|a_n(\zeta)|/dn) \approx -(\sqrt{3}/2)\zeta(3n - 12)^{-2/3}, \quad (23)$$

when $\exp(-\sqrt{3}\rho_n\zeta/2) \gg 1$. Equation (23) shows that the gain per pass decreases with increasing pass number n . Please see Ref. [13] for further discussions.

ACKNOWLEDGEMENTS

The author would like to acknowledge valuable discussions with T. Shizuma at JAERI, S. Hiramatsu at KEK, and H. Hama at Tohoku University.

REFERENCES

- [1] G. Dattoli and A. Renieri, in *Laser Handbook*, edited by M.L. Stitch and M. Bass (North Holland, Amsterdam, 1985), Vol.4, p.75.
- [2] N. Piovella et al., PRE **52**, 5470 (1995); P. Chaix et al., PRE **59**, 1136 (1999).
- [3] G. Dattoli and A. Renieri, Nuovo Cimento B **59**, 1 (1980); G. Dattoli et al., Opt. Comm. **35**, 407 (1980).
- [4] H. Al-Abawi et al., Opt. Comm. **30**, 235 (1979); J. G. Kuper et al., Opt. Comm. **34**, 117 (1980).

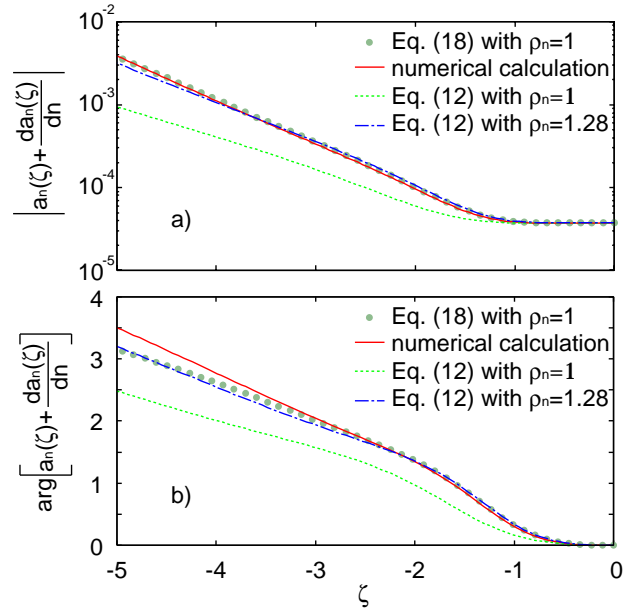


Figure 1: The amplitude (a) and phase (b) of the output field $a_n(\zeta) + \frac{da_n(\zeta)}{dn}$ as a function of ζ . The solid circles stand for the output field of the second pass given by Eq. (18) with $\rho_n = 1$, and the solid line is that obtained from a numerical calculation where Eq. (12) with $\rho_n = 1$, which is represented by the dotted line, is used as an input field envelope. The dash-dotted line expresses an approximated output field of the second pass given by Eq. (12) with $\rho_n = 1.28$. The amplitude of the front edge $|a_n(0)| = 3.7 \times 10^{-5}$ is used.

- [5] W.B. Colson, in *Laser Handbook*, edited by W.B. Colson, C. Pellegrini, and A. Renieri (North Holland, Amsterdam, 1990), Vol.6, pp. 115–193.
- [6] Nicola Piovella, PRE **51**, 5147 (1995).
- [7] N. Nishimori et al., PRL **86**, 5707 (2001); NIM A **483**, 134 (2002).
- [8] R. Nagai et al., NIM A **483**, 129 (2002).
- [9] R. Hajima et al., NIM A **475**, 270 (2001); *ibid.* **483**, 113 (2002).
- [10] Z.-W. Dong et al., NIM A **483**, 553 (2002).
- [11] Ryoichi Hajima and Ryoji Nagai, PRL **91**, 024801 (2003).
- [12] Nobuyuki Nishimori, PRST AB **8**, 100701 (2005).
- [13] Nobuyuki Nishimori, accepted for publication in PRE.
- [14] Norman M. Kroll and Wayne A. McMullin, PRA **17**, 300 (1978).
- [15] W. B. Colson et al., PRA **34**, 4875 (1986).
- [16] R. Bonifacio et al., Riv. Nuovo Cimento **13**, 9 (1990).
- [17] W.B. Colson and S.K. Ride, Phys. Lett. **76A**, 379 (1980).
- [18] Kwang-Je Kim, PRL **57**, 1871 (1986); NIM A **250**, 396 (1986).
- [19] N. Nishimori, R. Hajima, R. Nagai and E.J. Minehara, NIM A **507**, 79 (2003).